Polyfluorenes with Phosphonate Groups in the Side Chains as Chemosensors and Electroluminescent Materials

Gang Zhou, Gang Qian, Liang Ma, Yanxiang Cheng, Zhiyuan Xie, Lixiang Wang,* Xiabin Jing, and Fosong Wang

State Key Laboratory of Polymer Physics and Chemistry, Changchun Institute of Applied Chemistry, Chinese Academy of Sciences, Graduate School of Chinese Academy of Sciences, Changchun 130022, P. R. China

Received April 17, 2005; Revised Manuscript Received May 2, 2005

ABSTRACT: Polyfluorenes (**P1** and **P2**) with phosphonate groups in the side chains were designed and synthesized. Their absorption and photoluminescence spectra in solutions are solvent dependent and exhibit a red shift up to 14 and 6 nm, respectively, with increasing solvent polarity. The polymers are highly soluble in ethanol with a solution photoluminescence quantum yield of 0.74. Polymer **P2** in thin film cast from ethanol shows high intrachain order as revealed by red-shifted absorption spectrum and emission spectrum along with well-resolved vibronic structure. Both **P1** and **P2** are highly sensitive and selective Fe^{3+} sensory materials, and the sensitivity is much higher than that of model compounds **3** and **4**. The highest sensitivity was observed with polymer **P1**, and a 210-fold fluorescence quenching in dichloromethane was achieved. Polymer light-emitting diodes (PLEDs) were also fabricated to investigate the electroluminescent properties. A luminous efficiency of 1.49 cd/A with Commission Internationale de L'Eclairage (CIE) coordinates of (0.171, 0.131) at 100 cd/m^2 and a maximum brightness of 1750 cd/m^2 have been demonstrated.

Introduction

Fluorescent conjugated polymers (CPs) have attracted much attention because of their potential optoelectronic and biological applications, such as light-emitting diodes,[1] photovoltaic devices,[2] field-effect transistors,[3] nonlinear optics,[4] and chemical and biological sensors.[5] Of all CPs, polyfluorenes (PFs) are one class of the most promising materials due to their high photoluminescence quantum yield, high thermal and chemical stability, and facile modification at the side chains without affecting main-chain conjugation.[6−11] CPs carrying ionic groups or special receptors can be used in detecting bioactive species[12−18] or offer some new opportunities in optoelectronics[19−23] and supramolecular chemistry.[24] Polyfluorenes with various functional groups, such as ammonium groups,[25] sulfonic groups,[26] phenol groups,[27] and imidazole groups,[28] have been reported. Among those the polymers with phenol groups and imidazole groups are highly sensitive and selective chemosensors for F^- and Cu^{2+}, respectively. PFs carrying ionic groups are soluble in alcohol or water and have been used to fabricate multilayer PLEDs or as the electron injection layer to improve the performance of PLEDs.[19−21]

The phosphine oxide groups are widely used in the preparation of quantum dots due to their strong affinity for inorganic nanocrystals.[29] While the amphiphilic phosphonate groups have been studied as surfactants[30] and receptors,[31,32] they have also successfully been introduced into the CPs, such as poly(*p*-phenylene ethynylene)[24,33] and polythiophene,[34] as the precursor for polymers with phosphonic acid groups. Introduction of the phosphonate groups into PFs may endow the polymers unique properties, for example, high solubility in polar solvents and sensing properties to certain metal ions. In current paper, we design and synthesize novel fluorene homopolymers with phosphonate groups in the side chains, and their optical properties, sensing properties, and electroluminescent properties are investigated.

* Corresponding author: lixiang@ciac.jl.cn, Fax: 0086-431-5685653.

Results and Discussion

Synthesis and Structure Characterization. Structures of the polymers and model compounds are depicted in Chart 1. The syntheses of monomers, polymers, and model compounds **3** and **4** are shown in Scheme 1. Our synthesis began with 2,7-dibromofluorene as described by Xia et al.[35] The reaction of 2,7-dibromofluorene with 1,3-dibromopropane in the presence of NaOH aqueous solution afforded 2,7-dibromo-9,9-bis(3′-bromopropyl)-fluorene in a yield of 62% after purification with columnar chromatography. The main byproduct was 2,7-dibromo-9-cyclobutylfluorene in a yield of 21%. Then 2,7-dibromo-9,9-bis(3′-diethoxylphosphorylpropyl)-fluorene (**1**) was obtained as white crystal in a yield of 91% by refluxing 2,7-dibromo-9,9-bis(3′-bromopropyl)-fluorene in triethyl phosphite. The monomer 2,7-dibromo-9,9-bis(6′-diethoxylphosphorylhexyl)fluorene (**2**) was obtained in the same way as colorless oil in a yield of 83%. The polymerization reactions of monomers **1** and **2** via the Yamamoto polycondensation[36] reaction with Ni(0) as the catalyst produced light-yellow fibers of **P1** and **P2** after repeated dissolution in chloroform and precipitation in *n*-hexane in the yields of both over 50%. Models **3** and **4** were prepared through Suzuki coupling reaction between monomers **1** and **2** and 2-(9,9-dioctyl-fluoren-2-yl)-4,4,5,5-tetramethyl-[1,3,2]dioxaborolane with $Pd(PPh_3)_4$ as the catalyst. They were both obtained as yellowish oil in a yield of over 60%.

Structures of polymers **P1** and **P2** were verified by FT-IR, ^{1}H NMR, and elemental analysis. We could not measure the molecular weight of **P1** and **P2** by normal gel permeation chromatography (GPC) method due to strong absorption of the polymers on the column fillers possibly induced by the high polarity of the phosphonate

10.1021/ma050807h CCC: $30.25
Published on Web 05/27/2005

Chart 1. Structures of Polymers and Model Compounds

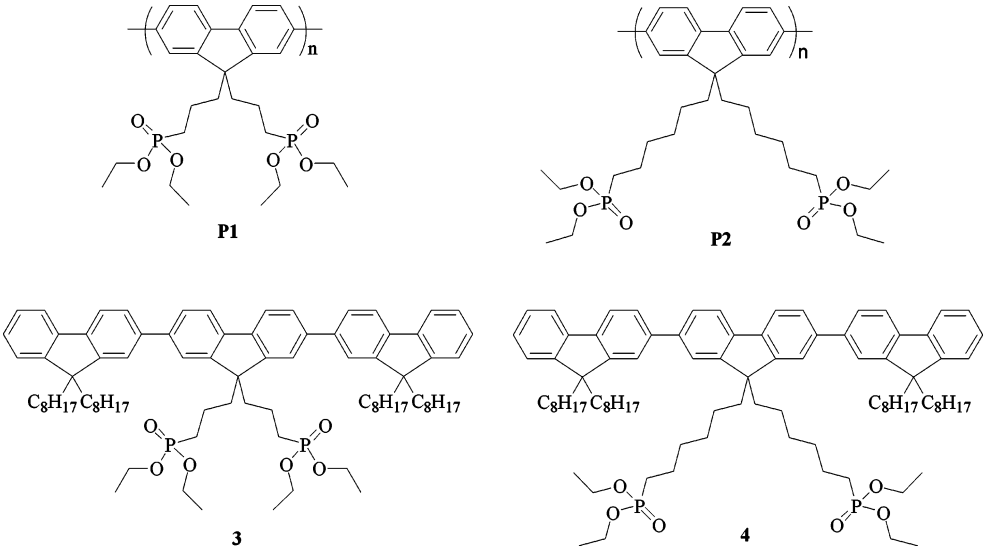

Scheme 1. General Synthetic Scheme for the Preparation of Compounds 1−4 and Polymers P1 and P2[a]

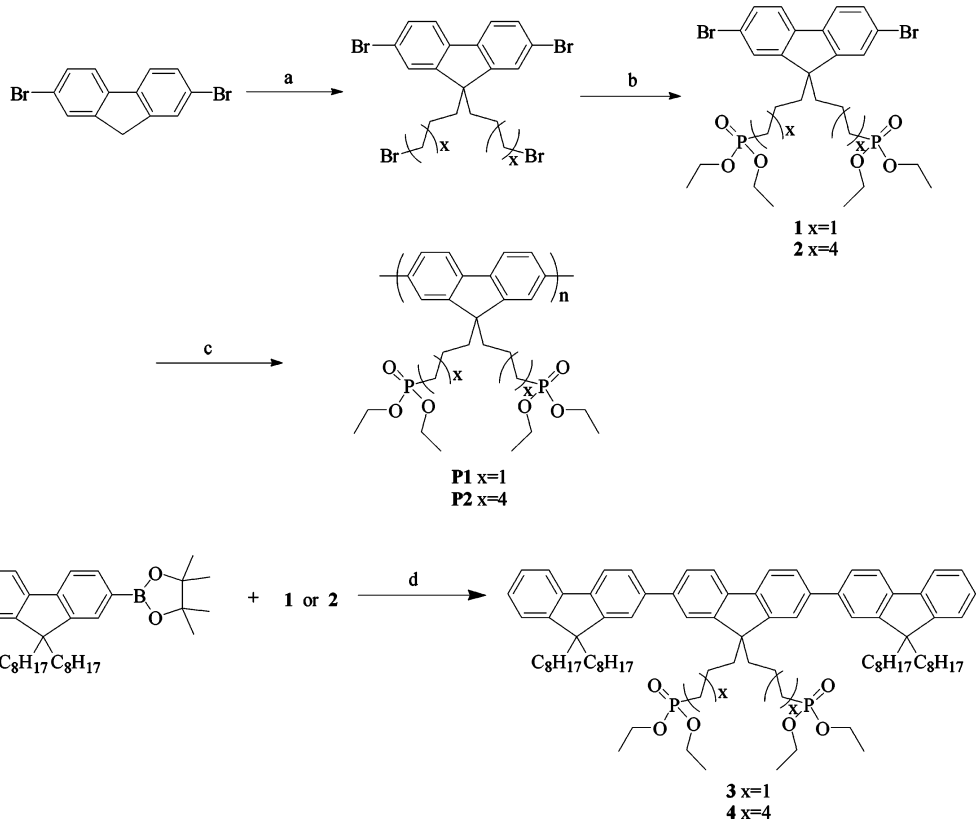

[a] (a) 1,3-Dibromopropane or 1,6-dibromohexane, $NaOH/H_2O$, 60 °C, 4 h; (b) triethyl phosphite, 140 °C, 16 h; (c) Ni(0), toluene/DMF, 80 °C, 96 h; (d) $Pd(PPh_3)_4$, Na_2CO_3, toluene/H_2O, 80 °C, 24 h.

groups. Then the molecular weights of **P1** and **P2** were estimated to be 25−35 kDa by comparing their viscosity[37] in chloroform with poly(9,9-dioctylfluorene) (**PF8**, M_n = 32 kDa); however, the error may be significant due to the different polarity between these polymers and **PF8**.

The thermal properties of polymers **P1** and **P2** were studied by thermogravimetric analysis (TGA) (Figure 1). A moderate weight loss (about 3%−4%) starts from 100 °C, which is obviously due to releasing the associated water,[20,23] although the polymers were dried in a vacuum at 100 °C for 1 day before the measurements. In a nitrogen atmosphere, polymers **P1** and **P2** exhibit a degradation onset at 225 and 194 °C, respectively, which are contributed to the decomposition of phosphonate groups. Another significant degradation starts over 300 °C, corresponding to the cleavage of alkyl side chains. Unlike typical poly(9,9-dialkylfluorene)s (PAFs),[38] differential scanning calorimetry (DSC) measurements did not show any phase transition, and no clear mesophase was observed under polarizing optical microscopy (POM).

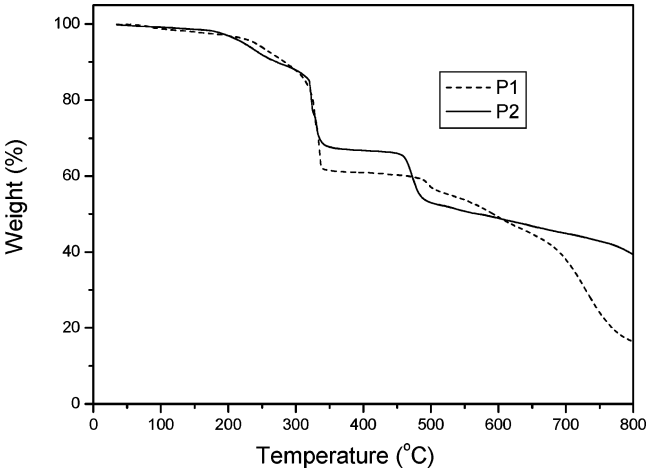

Figure 1. Thermalgravimetric analysis curves of polymers **P1** and **P2**.

Optical Properties. Polymers **P1** and **P2** are soluble in most of common organic solvents, such as tetrahydrofuran (THF), toluene, dimethylformamide (DMF), chloroform ($CHCl_3$), and dimethyl sulfoxide (DMSO). Especially, they are also highly soluble in methanol, ethanol, and acetone. The solubility of either **P1** or **P2** in ethanol is over 10 mg/mL. The quantum yield of **P1** and **P2** in dilute solution (ca. 10^{-6} M of repeat unit) is almost the same. With 9,10-diphenylanthracene as a standard, the quantum yields of **P2** in ethanol and chloroform are 74% and 93%, respectively. These values are significantly higher than the photoluminescence (PL) quantum yield of fluorene derived polyelectrolytes.[20,23] The absorption and photoluminescence spectra in solution were measured at a concentration of ca. 10^{-5} M of repeat unit. Like fluorene derived polyelectrolytes,[20,23] the solution absorption and PL spectra of **P1** and **P2** are dependent on the solvent. **P1** shows the absorption maximum at 382 nm in chloroform, 388 nm in ethanol, 391 nm in DMF, and 392 nm in DMSO, while the corresponding PL spectra of **P1** are peaked at 417, 418, 422, and 423 nm with the vibronic shoulder around 438, 440, 443, and 444 nm, respectively (Figure 2a). The absorption maximum of **P2** in chloroform, ethanol, DMF, and DMSO is at 392, 401, 400, and 406 nm, respectively, while the emission bands are peaked at 418, 422, 423, and 424 nm with vibronic shoulder around 442, 436, 445, and 438 nm, respectively (Figure 2b). Since no aggregation absorption or excimer emission was observed, we attribute this red shift to enhanced chain conjugation driven by strong interaction between phosphonate groups and solvent molecules in polar solvents. Absence of aggregation is also evidenced by relatively high photoluminescence quantum yield of both polymers in ethanol.

The thin films of **P1** and **P2** were fabricated by spin-casting their chloroform or ethanol solutions (10 mg/mL) onto quartz substrates. The films from DMF and DMSO solutions were not studied here due to the high boiling point of the solvents. The absorption maxima of the thin films of **P1** and **P2** cast from chloroform solutions are at 381 and 388 nm, respectively, while the PL spectra have two peaks at 428 and 450 nm for **P1** and 434 and 453 nm for **P2** (Figure 3). Thin film absorption maxima of **P1** and **P2** cast from ethanol solutions further red-shift to 388 and 403 nm, but almost the same as solution spectra. Thin film PL spectrum of **P1** cast from ethanol solution is identical

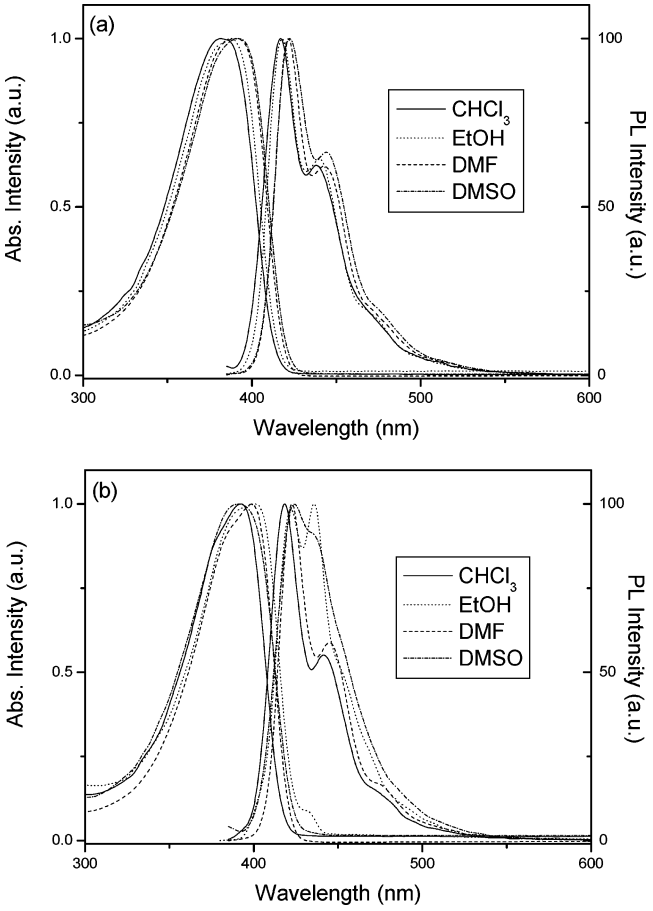

Figure 2. UV−vis absorption and PL spectra of **P1** (a) and **P2** (b) in $CHCl_3$, EtOH, DMF, and DMSO.

to that cast from chloroform solution, whereas that of **P2** cast from ethanol solution shows a 3−9 nm further red shift with major peak at 437 nm and two clear vibronic shoulders at 460 and 490 nm. Obviously, the PL spectrum of **P2** is better resolved. All these indicate that polymer chain of **P2** is well ordered in film cast from ethanol. Similar PL spectral features are also observed in annealed or solvent vapor-treated PFO films[39] and a rod−coil fluorene copolymer.[40] The authors attributed this spectral red shift to improved intrachain order or longer effective conjugation length. Figure 4 shows absorption and PL spectra of **P2** cast from chloroform solution before and after annealing at 100 °C. After annealing, a 12 nm red shift for absorption maximum and a 6 nm red shift for PL spectrum with better-resolved peaks were observed, indicating that polymer chains of **P2** prefer higher intrachain order in solid state.[39,40] Under the same treatment, **P1** exhibits a 3 nm red shift for absorption maximum and a 5 nm red shift for PL spectrum. The sky blue emission color of the films cast from ethanol solutions of polymer **P1** or **P2** is almost unchanged with a less than 15% reduction of PL intensity after heat treatment at 100 °C for 1 h in a vacuum. Compared with the PL spectra in dilute solutions, film PL spectra show a red shift up to 16 nm with slightly changed absorption maximum. The optical change from a dilute solution to thin film have also been observed in Yang's BDOH-PF.[41]

Sensing Properties. The sensing properties of polymers **P1** and **P2** to different metal ions were characterized in 5 μM dichloromethane (CH_2Cl_2) solutions. Upon addition of metal ions, i.e., Li^+, Na^+, K^+, Mg^{2+}, Ca^{2+},

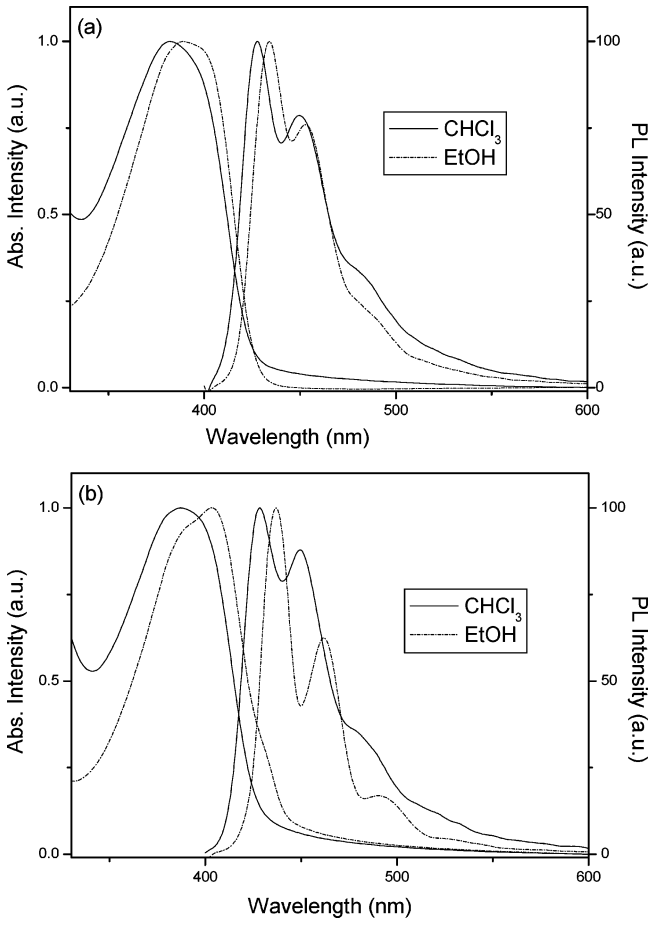

Figure 3. UV−vis absorption and PL spectra of **P1** (a) and **P2** (b) films cast from chloroform and ethanol solutions.

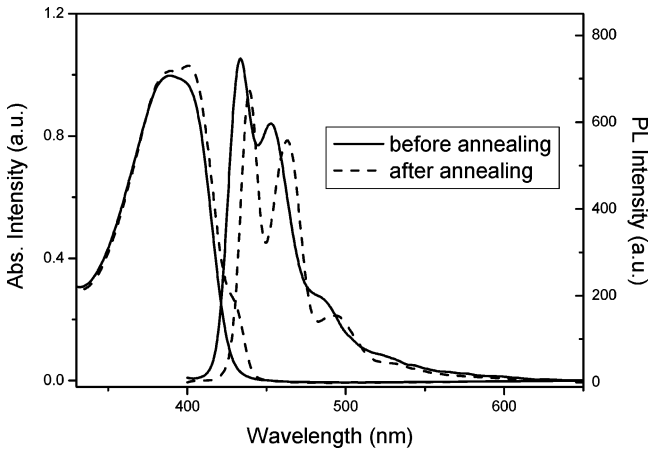

Figure 4. UV−vis absorption and PL spectra of **P2** film cast from chloroform solution before and after annealing at 100 °C for 1 h.

Sr^{2+}, Cd^{2+}, Mn^{2+}, Fe^{2+}, Cu^{2+}, Co^{2+}, Ni^{2+}, Ag^{+}, Zn^{2+}, and Pb^{2+}, no obvious changes of absorption spectra were observed, while the addition of Fe^{3+} caused an obvious enhancement of the molar extinction coefficient (ϵ) of **P1** at short wavelength along with a slight increase around main absorption band, as shown in Figure 5a. **P2** showed identical behavior. In contrast, the response of fluorescence spectra of the polymers to the addition of Fe^{3+} ion was much remarkable. When the Fe^{3+} ion was added into the CH_2Cl_2 solution of **P1** (Figure 5b), the emission intensity decreased dramatically with a fluorescence quenching up to 210-fold. The addition of

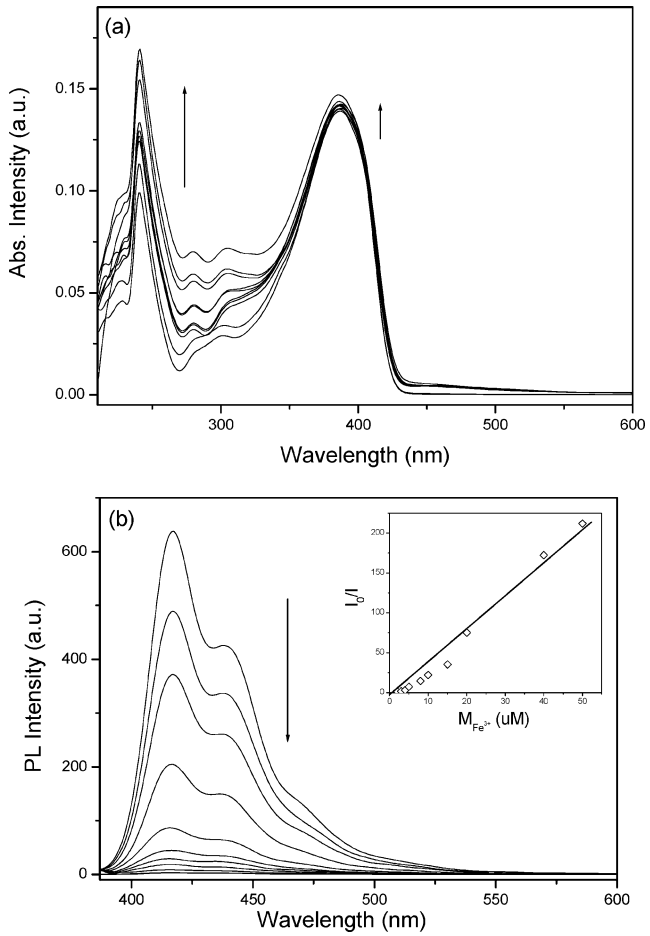

Figure 5. Absorption (a) and fluorescence (b) spectra of **P1** in CH_2Cl_2 solution upon addition of Fe^{3+}. The Stern−Volmer plots are shown as an inset.

Fe^{3+} to the CH_2Cl_2 solution of **P2** also led to a 130-fold reduction in emission intensity. From the Stern−Volmer plots as an inset of Figure 5b, the corresponding Stern−Volmer constants (K_{sv}) were calculated to be 4.05×10^6 and 2.24×10^6 for **P1** and **P2**, respectively. Since adding Fe^{3+} ion into poly(9,9-dioctylfluorene) (PF8) solution only led to an emission reduction less than 5-fold, we tentatively attribute the high sensitivity of polymers **P1** and **P2** to Fe^{3+} to the formation of certain complex between Fe^{3+} ions and phosphonate groups, which can quench the emission from the polymers. The different sensitivity between **P1** and **P2** is probably due to the different length of the alkyl chains, which results in different distance between Fe^{3+}−phosphonate group quencher and the polymer backbone.[42]

Fluorescence emission response profiles of polymers **P1** and **P2** in CH_2Cl_2 solution upon addition of other metal ions were also investigated, as shown in Figure 6. Almost all the metal ions have no effects on the fluorescence spectra of polymers **P1** and **P2**, except that Cu^{2+} and Mg^{2+} result in slight fluorescence quenching of less than 15-fold and 5-fold, respectively. These results indicate that polymers **P1** and **P2** are both highly sensitive and selective chemosensors for the Fe^{3+} ion.

Sensing properties of the polymers to Fe^{3+} ion were also studied in different solvents. As shown in Figure 7, the fluorescence intensity of **P1** in tetrahydrofuran (THF) solution (5 μM) was almost quenched after the addition of 100 μM Fe^{3+} ion. However, when a drop of

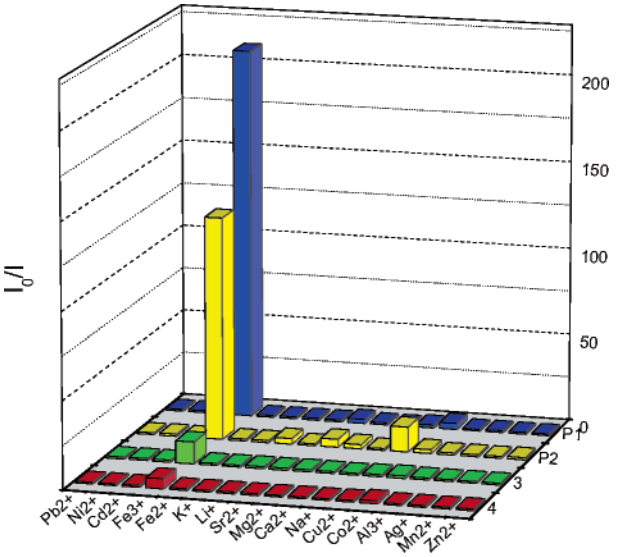

Figure 6. Fluorescence response profiles of **P1**, **P2** and **3**, **4** in CH_2Cl_2 upon addition of different metal ions.

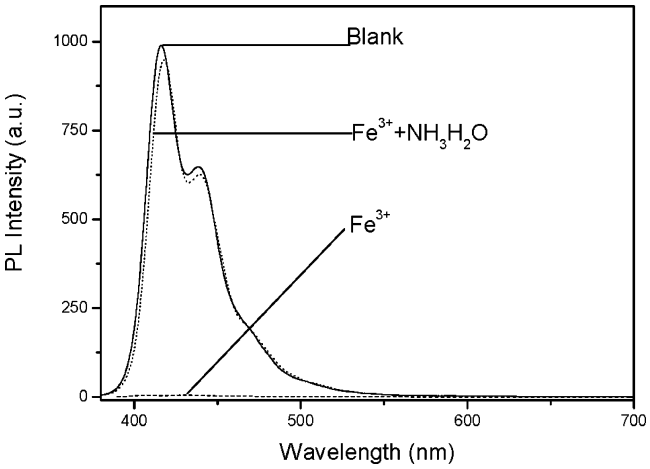

Figure 7. Fluorescence spectra of polymer **P1** in THF with or without presence of Fe^{3+} and $NH_3{\cdot}H_2O$.

ammonia solution (14 M concentration) was added to the solution, the fluorescence spectrum was recovered to that before adding analyte. When the experiment was performed with polymer **P2**, a similar phenomenon was also observed. This result indicates that the sensing properties of the polymers are originated from the certain interaction between Fe^{3+} ions and the phosphonate groups, and polymer **P1** and **P2** can act as reversible chemosensors for the Fe^{3+} ion.

Fluorescence emission response profiles of polymers **P1** and **P2** in ethanol solution upon addition of various metal ions are exhibited in Figure 8. Similar to the case in CH_2Cl_2, sensitivity of the polymers to the most of metal ions is very low except for Fe^{3+}. When excess Fe^{3+} (100 μM) was added into the ethanol solution of polymers **P1** and **P2**, the fluorescence intensity of polymers **P1** and **P2** only drop 18-fold and 14-fold, respectively. The corresponding K_{sv} values were determined to be 3.55×10^5 and 2.71×10^5, respectively. The decreased quenching effect should be attributed to the hydrogen-bonding interactions between the ethanol molecules and the phosphonate groups, which weakens the interactions between the receptors and the analytes. This behavior was also observed in PFs for sensing F^-.[27]

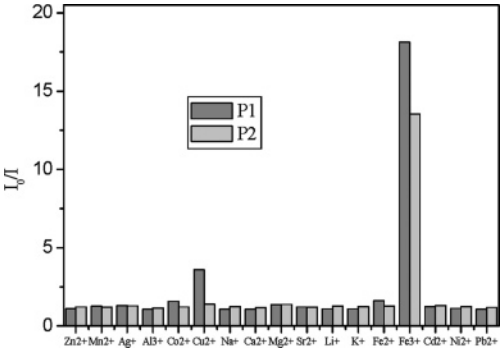

Figure 8. Fluorescence response profiles of **P1** and **P2** in ethanol upon addition of different metal ions.

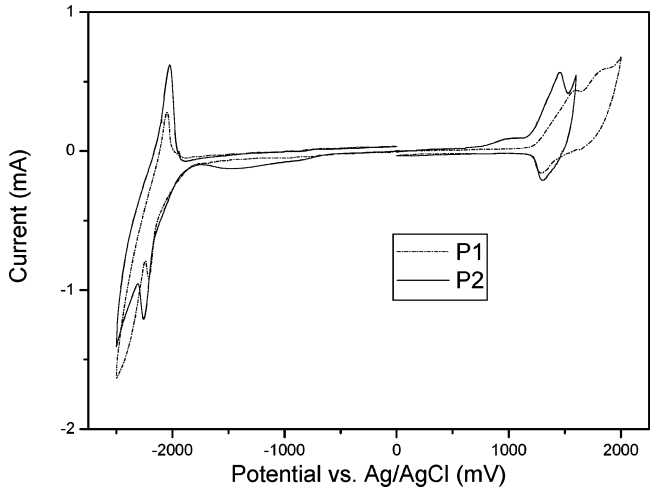

Figure 9. Cyclic voltammograms of the **P1** and **P2** films coated on platinum electrodes in 0.1 M Bu_4ClO_4 CH_3CN solution.

To investigate the amplification effect[43] of conjugated polymer chain, model compounds **3** and **4** were synthesized and studied. Upon addition of excess Fe^{3+} (1 mM) to the CH_2Cl_2 solution of **3** and **4**, the fluorescence intensity only quenched up to 12-fold and 6-fold, respectively (Figure 6). The corresponding K_{sv} values were determined to be 1.14×10^5 and 5.83×10^4, respectively. Both the quenching effects and K_{sv} values are much lower than those of polymers, which once more proves signal amplification ability of conjugated polymers due to facile energy migration along the polymer backbone.[5]

Electrochemical Properties. The electrochemical behaviors of the polymers **P1** and **P2** were investigated by cyclic voltammetry (CV), as shown in Figure 9. The CV was performed in a solution of Bu_4NClO_4 (0.1 M) in acetonitrile at a scan rate of 50 mV/s at room temperature under argon with an Ag/Ag^+ electrode as the reference electrode. A platinum electrode coated with a thin polymer film was used as the working electrode. According to the onset potential of the oxidation process and reduction process, we estimate the highest occupied molecular orbital (HOMO) and the lowest unoccupied molecular orbital (LUMO) energy levels of the polymer **P1** to be −5.5 and −2.2 eV with the formula ($E_{HOMO} = -(E^{ox} + 4.34)$ eV and $E_{LUMO} = -(E^{red} + 4.34)$ eV).[44] Compared with the HOMO (−5.8 eV)[45] level of PAF, 0.3 eV reduced HOMO level of **P1** should be attributed to the effect of phosphonate groups on the polymer side chains. This phenomenon was also observed in fluorene-based polyelectrolytes.[20] There are no obvious differences in the HOMO and LUMO levels between polymer

Table 1. EL Emission Maximum (λ_{max}), Turn-On Voltage (V_T), Maximum Brightness (B_{max}), Luminous Efficiency (η_c), and CIE Coordinates of the Polymers P1 and P2 with a Device Structure of ITO/HTL/P1 or P2/Ca/Al

device	polymers/solutions	HTL	λ_{max} (nm)	V_T (V)	B_{max} (cd/m^2)	η_c[a] (cd/A)	CIE[a]
1	**P1**/$CHCl_3$	PEDOT	424, 448 (sh)[b]	6.0	901	0.22	0.172, 0.167
2	**P2**/$CHCl_3$	PEDOT	428, 452 (sh)	4.5	2779	1.25	0.177, 0.230
3[c]	**P1**/$CHCl_3$	PEDOT	424, 448 (sh)	5.0	1279	0.19	0.173, 0.099
4[c]	**P2**/$CHCl_3$	PEDOT	436, 460 (sh)	4.0	4101	0.34	0.158, 0.074
5	**P1**/EtOH	PEDOT	424, 448 (sh)	4.5	520	0.10	0.167, 0.138
6	**P2**/EtOH	PEDOT	436, 460 (sh)	5.0	1160	0.63	0.164, 0.088
7	**P1**/EtOH	PVK	420, 448 (sh)	6.0	883	0.29	0.175, 0.142
8	**P2**/EtOH	PVK	436, 460 (sh)	7.5	1750	1.49	0.171, 0.131

[a] At a brightness of 100 cd/m^2. [b] Shoulder peak. [c] After heat treatment at 100 °C for 1 h in a vacuum.

P1 and **P2** due to the same main-chain structure and the same end phosphonate side groups. From the electrochemical data we estimate that the band gap is around 3.3 eV, which is significantly larger than the optical band gap 2.8 eV estimated from absorption onset at 430 nm. The band gap difference of PAFs measured by optical and electrochemical methods was previously reported by Janietz et al.;[45] no detailed explanation about the discrepancy was provided in their paper.

Electroluminescent Properties. To test electroluminescent properties of polymers **P1** and **P2**, devices with two different configurations were fabricated, i.e., ITO/poly(3,4-ethylenedioxythiophene)−poly(styrenesulfonic acid) (PEDOT−PSS, 50 nm)/polymer (50 nm)/Ca (10 nm)/Al (100 nm) and ITO/poly(vinylcarbazole) (PVK, 50 nm)/polymer (50 nm)/Ca(10 nm)/Al(100 nm). Ethanol was chosen as the spin-coating solvent for **P1** and **P2** in all devices, except that chloroform was also used in fabrication of the first type of devices for comparison. High solubility of the polymers **P1** and **P2** in alcohol makes the preparation of the second type of devices possible by means of spin-coating without interface interference. The device performance measured under ambient conditions is listed in Table 1. The EL maxima of both **P1** and **P2** are identical to those of PL spectra. With PVK as the hole-transporting layer (HTL), the diodes with **P1** and **P2** as emitting layer show the luminous efficiencies of 0.29 and 1.49 cd/A with the Commission Internationale de L'Eclairage (CIE) coordinates of (0.175, 0.142) and (0.171, 0.131) at 100 cd/m^2 and the maximum brightness of 883 and 1750 cd/m^2, respectively. With PEDOT−PSS as the HTL, the devices fabricated from ethanol exhibit the poorest efficiency, but the better color purity, indicated by CIE coordinates of (0.167, 0.138) for **P1** and (0.164, 0.088) for **P2**. The devices with PEDOT−PSS as the HTL fabricated from chloroform exhibit the luminous efficiency close to that of the devices with PVK as the HTL; however, the color purity is very poor. The EL spectra of **P2** with different fabrication conditions at the driving voltage of 10 V are shown in Figure 10. For all spectra, a well-resolved emission structure with peaks at 436, 460, and 490 nm, assigned to the 0−0, 0−1, and 0−2 intrachain singlet transitions,[46] respectively, was observed. Both types of devices with ethanol as the device fabrication solvent afford clean and typical EL spectra of PFs. The poorest color purity of **P2** with PEDOT−PSS as the HTL and chloroform as the spin-coating solvent, indicated by CIE coordinates, is attributed to the more pronounced emission from 0−2 and 0−3 transitions. However, after heat treatment of this device at 100 °C for 1 h in a vacuum, a red shift for EL spectra was observed, like that occurring in PL spectra (Figure 11). Most importantly, the emission from 0−2 and 0−3 transitions was depressed, and then the color

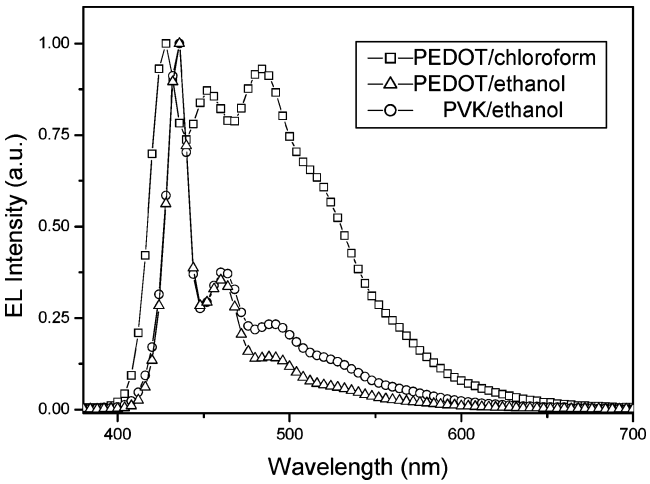

Figure 10. Electroluminescence spectra of **P2** with PEDOT−PSS and PVK as hole-transporting layer at a driving voltage of 10 V.

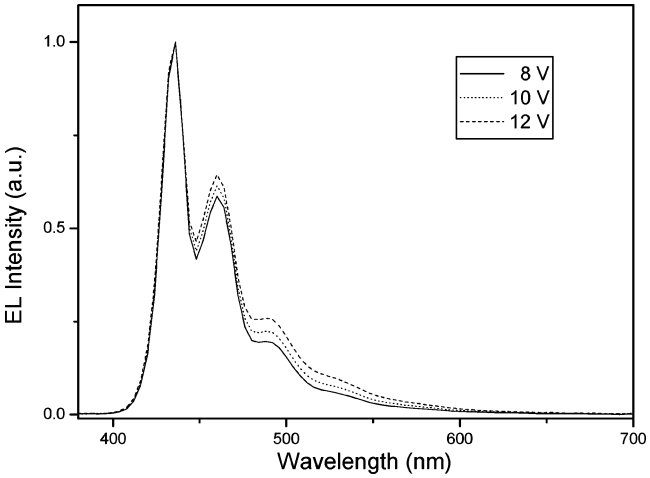

Figure 11. EL spectra of device ITO/PEDOT/**P2**(chloroform)/Ca/Al after heat treatment at 100 °C for 1 h in a vacuum under different driving voltages.

purity was significantly improved, as indicated by the CIE coordinates in Table 1. Moreover, the EL spectra are insensitive to driving voltage. As shown in Figure 11, with increasing the driving voltage from 8 to 12 V, the EL spectra are almost same. The CIE coordinates under driving voltages of 8, 10, and 12 V are (0.158, 0.079), (0.159, 0.090), and (0.161, 0.103), respectively, corresponding to the brightness of 433, 741, and 1082 cd/m^2. We did not observe a featureless green emission band in the EL spectra of **P1** and **P2**, which often appears in PFs EL devices. We speculate that phosphonate groups surrounding the main chain might be able to suppress the interchain interaction of the current polymers and therefore to prevent the formation of

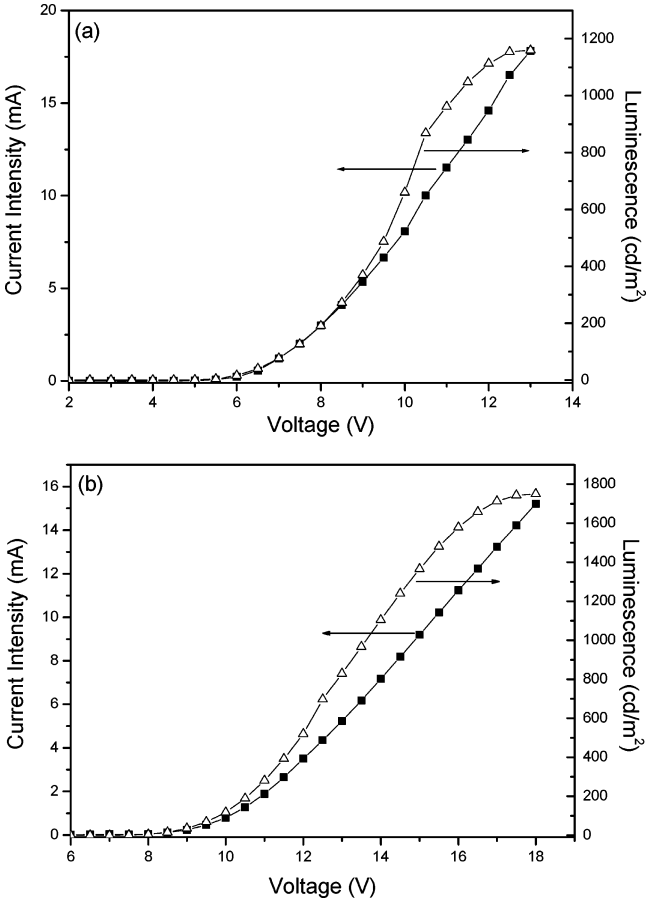

Figure 12. $I-V$ and $L-V$ curves of device from **P2** with PEDOT (a) and PVK (b) as the HTL.

excimer or aggregation. Figure 12a,b shows the $I-V$ and $L-V$ curves of devices from **P2** with PEDOT-PSS and PVK as the HTL and ethanol as the solvent. The relatively higher turn-on voltage of the devices with PVK as the HTL should be attributed to the large hole-injection barrier owing to the low HOMO level of PVK, which should be improved by choosing appropriate triarylamine compounds as the HTL or inserting a hole injection layer. In PLEDs fabrication, the polymer layers are generally deposited through the solution process; thus, the hole-transporting materials need to be solvent resistant to enable the fabrication of the subsequent layer. As the dominant hole-transporting materials nowadays, PEDOT−PSS involves over amount of sulfonic acid groups and is strongly hydrophilic, which might be disadvantageous in terms of device stability. Several cross-linkable hole-transporting materials based on triarylamine have been developed to replace PEDOT−PSS.[47,48] Since most of triarylamine hole-transporting materials are insoluble in alcoholic solvents and water, the development of the emitting polymers soluble in these solvents should provide the other approach to avoid the disadvantages of PEDOT−PSS.

In summary, we have successfully synthesized polyfluorenes with phosphonate polar groups in the side chains. A red shift of the absorption and PL spectra in solutions was distinctly observed with increasing solvent polarity. Polymer **P2** shows high intrachain order in film spin-cast from ethanol, revealed by both red-shifted absorption and emission along with better-resolved emission spectra. Both polymers show high photoluminescence quantum yield in ethanol. The polymers are highly sensitive and selective chemosensory materials for Fe^{3+} with an emission quenching up to 210-fold upon addition of Fe^{3+}. Blue PLEDs was successfully fabricated with PVK as the HTL through solution process. A luminous efficiency of 1.49 cd/A with the CIE coordinates of (0.171, 0.131) at 100 cd/m^2 has been demonstrated. In addition to the sensing properties, the polymers with phosphonate groups may also provide the possibility for selecting wide range of hole-transporting materials in PLEDs fabrication.

Experimental Section

Measurement and Characterization. ^{1}H and ^{13}C NMR spectra were recorded with Varian XL-300 NMR chloroform-*d* as solvents and tetramethylsilane as internal standard. The elemental analysis was performed on a Bio-Rad elemental analysis system. Mass spectroscopic analysis was recorded on a matrix-assisted laser desorption ionization time-of-flight mass spectrometer LDI-1700 (American Linear Scientific Inc.). Differential scanning calorimetry (DSC) and thermal gravimetric analysis (TGA) were performed under a nitrogen atmosphere at a heating rate of 10 °C min^{-1} through the use of Perkin-Elmer-DSC 7. Polarizing optical microscopy (POM) measurements were performed with a Leica optical microscope (Leica Microsystems, Germany) in reflection mode with a CCD camera attachment. Cyclic voltammograms of polymer films were recorded on an EG&G 283 (Princeton Applied Research) at room temperature.

Fluorescence Titration Procedure. Fluorescence spectra were obtained on a Perkin-Elmer LS 50B luminescence spectrometer with xenon discharge lamp excitation. Measurements of UV−vis absorption spectra were carried out on a Perkin-Elmer Lambda 35 UV−vis spectrometer. Solutions of polymers **P1**, **P2** and models **3**, **4** were dilute at a concentration of 5×10^{-6} M (the concentration of polymers is based on the moles of the repeated unit) in CH_2Cl_2. Solutions of cationic perchlorate salts or cationic nitrate salts with the concentration of typically 5×10^{-4} M were prepared by successive dilution. Fluorescence titration was carried out by sequentially adding 0.1 mL aliquots of cation solutions in CH_2Cl_2 to 5.00 mL of the polymer solutions, and CH_2Cl_2 was added to acquire 10.00 mL of solutions. The solutions were stirred for 5 min prior to obtaining fluorescence spectra.

PLED Fabrication and Characterization. Polymers **P1** and **P2** were dissolved in ethanol and filtered through a 0.45 μm filter. Patterned indium tin oxide (ITO)-coated glass substrates were cleaned with ethanol, detergent, distilled water, and ethanol. After dried at 110 °C for half an hour, poly(3,4-ethylenedioxythiophene) (PEDOT) doped with poly(styrenesulfonic acid) (PSS) (Baytron-P 4083, Bayer AG) was spin-coated onto the anode followed by drying at 110 °C for half an hour. Poly(vinylcarbazole) (PVK) (Acros) and electroluminescent polymers **P1** and **P2** are successively coated onto the substrate. Film thickness was determined by ellipsometry (AUEL-III, Xi'an, China) as well as by applying a scratch to the polymer film and subsequent atomic force microscopy (AFM) (SPI3800N, Seiko Instruments Inc., Japan) imaging in the vicinity of the scratch. Ca and Al layers were thermally evaporated onto the emissive layer under a vacuum at a base pressure of 3×10^{-4} Pa. The electroluminescence (EL) spectra and current−voltage and brightness−voltage curves of devices were recorded using a Keithley 2400/2000 current/voltage source unit with a calibrated silicon photodiode under ambient conditions.

Material Synthesis. All chemicals and reagents were used as received from commercial sources without further purification. Solvents for chemical synthesis were purified according to standard procedures. All chemical reactions were carried out under an inert atmosphere. Intermediate 2-(9,9-dioctylfluoren-2-yl)-4,4,5,5-tetramethyl-[1,3,2]dioxaborolane[49] and 2,7-dibromofluorene[35] were synthesized as previously described.

2,7-Dibromo-9,9-bis(3′-bromopropyl)fluorene. A two-phase mixture of 2,7-dibromofluorene (5.0 g, 15 mmol), 1,3-dibromopropane (30 mL), tetrabutylammonium bromide (0.1 g), and sodium hydroxide (50% w/w) aqueous solution (30 mL) was stirred at 60 °C for 4 h under nitrogen. After diluting the reaction mixture with dichloromethane, the organic layer was washed with water and brine. The separated organic layer was dried over magnesium sulfate, and dichloromethane was evaporated. The nonreacted 1,3-dibromopropane was distilled in a vacuum, and 2,7-dibromo-9,9-bis(3′-bromopropyl)fluorene (5.4 g, 62%) was obtained as a white crystal by chromatography with petroleum ether as the eluent; mp 149−150 °C. ^{1}H NMR (300 MHz, $CDCl_3$) δ (ppm): 7.57 (d, 2H, J = 5.0 Hz), 7.52 (d, 2H, J = 4.6 Hz), 7.50 (s, 2H), 3.14 (t, 4H, J = 8.7 Hz), 2.15 (t, 4H, J = 8.2 Hz), 1.18 (m, 4H, J = 15.1 Hz). ^{13}C NMR (75 MHz, $CDCl_3$) δ (ppm): 144.96, 133.22, 125.23, 120.45, 116.24, 115.73, 48.75, 32.76, 27.87, 21.24. The compound 2,7-dibromo-9-cyclobutylfluorene (1.2 g, 21%) was separated as the main byproduct; mp 215−216 °C. ^{1}H NMR ($CDCl_3$) δ (ppm): 7.89 (s, 2H), 7.50 (m, 4H), 2.65 (t, 4H, J = 7.4 Hz), 2.43 (m, 2H, J = 11.1 Hz). ^{13}C NMR (75 MHz, $CDCl_3$) δ (ppm): 148.16, 131.57, 124.55, 120.46, 115.93, 115.15, 46.24, 27.24, 11.09.

2,7-Dibromo-9,9-bis(6′-bromohexyl)fluorene. A mixture of 2,7-dibromofluorene (5.0 g, 15 mmol), 1,6-dibromohexane (30 mL), tetrabutylammonium bromide (0.1 g), and sodium hydroxide (30 mL, 50% w/w) aqueous solution was stirred at 60 °C for 4 h under nitrogen. After diluting the reaction mixture with dichloromethane, the organic layer was washed with water and brine. The separated organic layer was dried over magnesium sulfate, and dichloromethane was evaporated. The nonreacted 1,6-dibromohexane was distilled in a vacuum, and 2,7-dibromo-9,9-bis(6′-bromohexyl)fluorene (8.3 g, 81%) was obtained as a white crystal by chromatography with petroleum ether as the eluent; mp 71−72 °C. ^{1}H NMR (300 MHz, $CDCl_3$) δ (ppm): 7.54 (d, 2H, J = 8.0 Hz), 7.47 (d, 2H, J = 8.0 Hz), 7.43 (s, 2H), 3.29 (t, 4H, J = 6.8 Hz), 1.93 (t, 4H, J = 8.3 Hz), 1.67 (m, 4H, J = 7.1 Hz), 1.20−1.05 (m, 8H), 0.58 (m, 4H, J = 8.0 Hz). ^{13}C NMR (75 MHz, $CDCl_3$) δ (ppm): 146.42, 133.32, 124.59, 120.35, 115.82, 115.47, 49.81, 34.27, 28.05, 26.86, 23.19, 21.99, 17.71.

2,7-Dibromo-9,9-bis(3′-diethoxylphosphorylpropyl)-fluorene (1). A solution of 2,7-dibromo-9,9-bis(3′-bromopropyl)fluorene (3.0 g, 5 mmol) in triethyl phosphite was heated to 140 °C for 16 h. Then the excess triethyl phosphite was distilled in a vacuum, and monomer **1** (3.3 g, 91%) was obtained as a white crystal after purification with chromatography (ethyl acetate as the eluent); mp 101−103 °C. ^{1}H NMR (300 MHz, $CDCl_3$) δ (ppm): 7.54 (d, 2H, J = 8.6 Hz), 7.51 (d, 2H, J = 6.4 Hz), 7.45 (s, 2H), 3.93 (m, 8H), 2.08 (m, 4H, J = 8.2 Hz), 1.50 (m, 4H), 1.20 (t, 12H, J = 7.0 Hz), 0.90 (m, 4H). ^{13}C NMR (75 MHz, $CDCl_3$) δ (ppm): 151.37, 139.47, 131,10, 126.52, 122.16, 121.85 (C-fluorene ring), 61.74 ($-OCH_2-$), 55.76 (C_9-fluorene ring), 41.04 ($-CH_2-$), 26.86 ($-CH_2-$), 25.00 ($-CH_2-$), 16.77 ($-CH_3$). Anal. Calcd for $C_{27}H_{38}Br_2O_6P_2$: C, 47.67; H, 5.63; Br, 23.49; P, 9.11. Found: C, 47.33; H, 5.79; Br, 23.84; P, 8.61. MS *m/z*: 680.7 (M^+).

2,7-Dibromo-9,9-bis(6′-diethoxylphosphorylhexyl)-fluorene (2). A solution of 2,7-dibromo-9,9-bis(6′-bromohexyl)fluorene (4.0 g, 6 mmol) in triethyl phosphite was heated to 140 °C for 16 h. Then the excess triethyl phosphite was distilled in a vacuum, and monomer **2** (3.9 g, 83%) was obtained as colorless oil after purification with chromatography (ethyl acetate as the eluent). ^{1}H NMR (300 MHz, $CDCl_3$) δ (ppm): 7.56 (d, 2H, J = 8.0 Hz), 7.49 (d, 2H, J = 8.2 Hz), 7.44 (s, 2H), 4.08 (m, 8H, J = 7.8 Hz), 1.93 (t, 4H, J = 8.2 Hz), 1.63 (m, 4H), 1.45 (m, 4H), 1.32 (t, 12H, J = 8.5 Hz), 1.13 (m, 8H), 0.61 (m, 4H).^{13}C NMR (75 MHz, $CDCl_3$) δ (ppm): 152.63, 139.44, 130.67, 126.47, 121.91, 121.58 (C-fluorene ring), 61.66 ($-OCH_2-$), 55.95 (C_9-fluorene ring), 40.53 ($-CH_2-$), 30.49 ($-CH_2-$), 29.72 ($-CH_2-$), 26.86 ($-CH_2-$), 25.00 ($-CH_2-$), 23.90 ($-CH_2-$), 13.87 ($-CH_3$). Anal. Calcd for $C_{33}H_{50}Br_2O_6P_2$: C, 51.84; H, 6.59; Br, 20.90; P, 8.10. Found: C, 51.12; H, 6.88; Br, 21.18; P, 7.39. MS *m/z*: 764.7 (M^+).

Poly(9,9-bis(3′-diethoxylphosphorylpropyl)fluorene) (P1). A mixture of $Ni(COD)_2$ (0.85 g, 3.0 mmol), 2,2′-dipyridine (0.25 g, 2.2 mmol), cyclooctadiene (0.35 g, 2.2 mmol), and DMF (5 mL) was heated to 80 °C for half an hour. Then a solution of **1** (0.34 g, 0.50 mmol) in 5 mL of toluene was added, and the reaction mixture was stirred at 80 °C for 4 days. After cooling to room temperature, the reaction mixture was poured into chloroform and washed with dilute HCl, water, and brine. The separated organic layer was dried over magnesium sulfate, and the solvent was evaporated. The product was obtained as a yellowish fiber (150 mg, 58%) after precipitation from hexane. ^{1}H NMR (300 MHz, $CDCl_3$) δ (ppm): 7.81 (b, 2H), 7.68 (b, 4H), 3.91 (b, 8H), 2.31 (b, 4H), 1.55 (b, 4H), 1.14 (b, 16H). IR (CaF_2), cm^{-1}: 2980 (m), 2938 (m), 2906 (m), 1738 (w), 1610 (w), 1459 (m), 1243 (s), 1055 (sh), 1027 (s), 957 (s), 816 (m). Anal. Calcd for $C_{27}H_{38}O_6P_2 \cdot H_2O$ (the amounts of water is based on the TGA analysis[20,23]): C, 60.22; H, 7.49; P, 11.49. Found: C, 59.87; H, 6.95; P, 10.68.

Poly(2,7-dibromo-9,9-bis(6′-diethoxylphosphoryl-hexyl)fluorene) (P2). A solution of $Ni(COD)_2$ (0.85 g, 3.0 mmol), 2,2′-dipyridine (0.25 g, 2.2 mmol), cyclooctadiene (0.35 g, 2.2 mmol), and DMF (5 mL) was heated to 80 °C for half an hour. Then a solution of **2** (0.38 g, 0.50 mmol) in 5 mL of toluene was added, and the reaction mixture was stirred at 80 °C for 4 days. After cooling to room temperature, the reaction mixture was poured into chloroform and washed with dilute HCl, water, and brine. The separated organic layer was dried over magnesium sulfate, and the solvent was evaporated. The product was obtained as a yellowish fiber (190 mg, 63%) after precipitation from hexane. ^{1}H NMR (300 MHz, $CDCl_3$) δ (ppm): 7.84 (b, 2H), 7.69 (b, 4H), 4.04 (b, 8H), 2.19 (b, 4H), 1.63 (b, 4H), 1.48 (b, 4H), 1.27 (b, 20H), 0.85 (b, 4H). IR (CaF_2), cm^{-1}: 2981 (sh), 2930 (s), 2857 (m), 1731 (m), 1607 (w), 1458 (m), 1401 (w), 1248 (s), 1030 (s), 957 (s), 815 (m). Anal. Calcd for $C_{33}H_{50}O_6P_2 \cdot H_2O$: C, 63.65; H, 8.42; P, 9.94. Found: C, 63.96; H, 7.89; P, 9.83.

9,9-Bis(3′-diethoxylphosphorylpropyl)-2,7-bis(9,9-di-*n*-octylfluorene-2-yl)fluorene (3). To a solution of **1** (0.68 g, 1 mmol) and 2-(9,9-dioctylfluoren-2-yl)-4,4,5,5-tetramethyl-[1,3,2]dioxaborolane (1.55 g, 3 mmol) in toluene (25 mL) was added $Pd(PPh_3)_4$ (10 mg) and 2 M aqueous Na_2CO_3 solution (15 mL). The mixture was degassed and stirred at 80 °C for 24 h and then was poured into a saturated solution of ammonium chloride and extracted with ethyl acetate; the combined organic layer was washed with brine and dried over Na_2SO_4. After removing the solvent, the residue was purified by column chromatography using ethyl acetate as eluent to give 0.90 g (69%) of yellowish oil. ^{1}H NMR (300 MHz, $CDCl_3$) δ (ppm): 7.80 (m, 6 H, Ar−H), 7.65 (m, 8 H Ar−H), 7.35 (m, 6 H, Ar−H), 3.92 (m, 8 H), 2.05 (m, 12 H), 1.56−1.08 (m, 56 H), 0.96−0.87 (m, 24 H). ^{13}C NMR (75 MHz, $CDCl_3$) δ (ppm): 151.92, 151.34, 150.55, 141.35, 141.17, 140.84, 140.66, 140.39, 132.58, 132.45, 129.00, 128.84, 127.42, 127.19, 126.51, 123.35, 121.76, 121.66, 120.68, 120.28, 120.12, 61.75, 55.61, 53.79, 41.25, 40.81, 32.17, 30.47, 29.64, 27.04, 25.19, 24.25, 22.98, 17.53, 16.72, 14.44. MS *m/z*: 1298.4 (M^+).

9,9-Bis(6′-diethoxylphosphorylhexyl)-2,7-bis(9,9-di-*n*-octylfluorene-2-yl)fluorene (4). To a solution of **2** (0.76 g, 1 mmol) and 2-(9,9-dioctylfluoren-2-yl)-4,4,5,5-tetramethyl-[1,3,2]dioxaborolane (1.55 g, 3 mmol) in toluene (25 mL) was added $Pd(PPh_3)_4$ (10 mg) and 2 M aqueous Na_2CO_3 solution (15 mL). The mixture was degassed and stirred at 80 °C for 24 h and then was poured into a saturated solution of ammonium chloride and extracted with ethyl acetate; the combined organic layer was washed with brine and dried over Na_2SO_4. After removing the solvent, the residue was purified by column chromatography using ethyl acetate as eluent to give 0.93 g (67%) of yellowish oil. ^{1}H NMR (300 MHz, $CDCl_3$) δ (ppm): 7.80 (m, 6H, Ar−H), 7.65 (m, 8H Ar−H), 7.35 (m, 6H, Ar−H), 4.05 (m, 8H), 1.95 (12H, m), 1.66−1.08 (m, 68H), 0.96−0.70 (m, 24H). ^{13}C NMR (75 MHz, $CDCl_3$) δ (ppm): 151.92, 151.87, 151.37, 141.15, 140.95, 140.82, 140.71, 140.38, 132.57, 132.44, 129.00, 127.42, 127.20, 126.93, 126.42, 123.35, 121.69, 120.66, 120.40, 120.31, 120.12, 61.91, 55.83, 40.99, 40.75, 32.17, 30.91, 30.69, 30.51, 30.41, 30.06, 29.58, 26.89, 25.03, 24.21, 24.11, 22.97, 16.84, 14.44. MS *m/z*: 1382.5 (M^+).

Acknowledgment. This work was supported by National Natural Science Foundation of China (Project No. 29992530 and 20174042) and 973 Project (2002CB613402).

References and Notes

(1) Müller, C. D.; Falcou, A.; Reckefuss, N.; Rojahn, M.; Wiederhirn, V.; Rudati, P.; Frohne, H.; Nuyken, O.; Becker, H.; Meerholz, K. *Nature (London)* **2003**, *421*, 829.
(2) Wohrle, D.; Meissner, D. *Adv. Mater.* **1991**, *3*, 129.
(3) Bao, Z.; Lovinger, A. J.; Brown, J. *J. Am. Chem. Soc.* **1998**, *120*, 207.
(4) Williams, D. J. *Angew. Chem., Int. Ed. Engl.* **1984**, *23*, 640.
(5) Swager, T. M. *Acc. Chem. Res.* **1998**, *31*, 201.
(6) Scherf, U.; List, E. J. W. *Adv. Mater.* **2002**, *14*, 477.
(7) Leclecr, M. *J. Polym. Sci., Part A: Polym. Chem.* **2001**, *39*, 2867.
(8) Wong, W. Y. *Coord. Chem. Rev.* **2005**, *249*, 971.
(9) Yu, W. L.; Pei, J.; Huang, W.; Heeger, A. J. *Adv. Mater.* **2000**, *12*, 828.
(10) List, E. J. W.; Guentner, R.; de Freitas, P. S.; Scherf, U. *Adv. Mater.* **2002**, *14*, 374.
(11) Lee, J.; Cho, H. J.; Jung, B. J.; Cho, N. S.; Shim, H. K. *Macromolecules* **2004**, *37*, 8523.
(12) Chen, L.; McBranch, D. W.; Wang, H. L.; Helgeson, R.; Wudl, F.; Whitten, D. G. *Proc. Natl. Acad. Sci. U.S.A.* **1999**, *96*, 12287.
(13) Heeger, P. S.; Heeger, A. J. *Proc. Natl. Acad. Sci. U.S.A.* **1999**, *96*, 12219.
(14) Wang, D.; Gong, X.; Heeger, P. S.; Rininsland, F.; Bazan, G. C.; Heeger, A. J. *Proc. Natl. Acad. Sci. U.S.A.* **2002**, *99*, 49.
(15) Gaylord, B. S.; Heeger, A. J.; Bazan, G. C. *Proc. Natl. Acad. Sci. U.S.A.* **2002**, *99*, 10954.
(16) Gaylord, B. S.; Heeger, A. J.; Bazan, G. C. *J. Am. Chem. Soc.* **2003**, *125*, 896.
(17) Wang, S.; Gaylord, B. S.; Bazan, G. C. *J. Am. Chem. Soc.* **2004**, *126*, 5446.
(18) Ho, H. A.; Boissinot, M.; Bergeron, M. G.; Corbeil, G.; Dore, K.; Boudreau, D.; Leclerc, M. *Angew. Chem., Int. Ed.* **2002**, *41*, 1548.
(19) Huang, F.; Hou, L.; Wu, H.; Wang, X.; Shen, H.; Cao, W.; Yang, W.; Cao, Y. *J. Am. Chem. Soc.* **2004**, *126*, 9845.
(20) Huang, F.; Wu, H.; Wang, D.; Yang, W.; Cao, Y. *Chem. Mater.* **2004**, *16*, 708.
(21) Wu, H.; Huang, F.; Mo, Y.; Yang, W.; Wang, D.; Peng, J.; Cao, Y. *Adv. Mater.* **2004**, *16*, 1826.
(22) Liu, B.; Yu, W.; Lai, Y.; Huang, W. *Chem. Commun.* **2000**, 551.
(23) Liu, B.; Yu, W.; Lai, Y.; Huang, W. *Macromolecules* **2002**, *35*, 4957.
(24) Pinto, M. R.; Kristal, B. M.; Schanze, K. S. *Langmuir* **2003**, *19*, 6523.
(25) Balanda, P.; Ramey, M.; Reynolds, J. *Macromolecules* **1999**, *32*, 3970.
(26) Fan, C.; Plaxco, K. W.; Heeger, A. J. *J. Am. Chem. Soc.* **2002**, *124*, 5642.
(27) Zhou, G.; Cheng, Y.; Wang, L.; Jing, X.; Wang, F. *Macromolecules* **2005**, *38*, 2148.
(28) Zhou, X.; Yan, J.; Pei, J. *Macromolecules* **2004**, *37*, 7078.
(29) Peng, X.; Schlamp, M. C.; Kadavanich, A. V.; Alivisatos, A. P. *J. Am. Chem. Soc.* **1997**, *119*, 7019.
(30) Edder, C.; Frechet, J. M. J. *Org. Lett.* **2003**, *5*, 1879.
(31) Molt, O.; Schrader, T. *Angew. Chem., Int. Ed.* **2003**, *42*, 5509.
(32) Wehner, M.; Schrader, T.; Finocchiaro, P.; Failla, S.; Consiglio, G. *Org. Lett.* **2000**, *5*, 605.
(33) Pinto, M. R.; Reynolds, J. R.; Schanze, K. S. *Polym. Prepr.* **2002**, *43*, 139.
(34) Stokes, K.; Heuze, K.; McCullough, R. *Macromolecules* **2003**, *36*, 7114.
(35) Xia, C.; Advincula, R. *Macromolecules* **2001**, *34*, 5854.
(36) Yamamoto, T. *Macromol. Rapid Commun.* **2002**, *23*, 583.
(37) Kim, S.; Jackiw, J.; Robinson, E.; Schanze, K.; Reynolds, J. *Macromolecules* **1998**, *31*, 964.
(38) Grell, M.; Bradley, D. D. C.; Inbasekara, M.; Woo, E. P. *Adv. Mater.* **1997**, *9*, 798.
(39) Grell, M.; Bradley, D. D. C.; Ungar, C.; Hill, J.; Whitehead, K. S. *Macromolecules* **1999**, *32*, 5810.
(40) Marsitzky, D.; Klapper, M.; Müllen, K. *Macromolecules* **1999**, *32*, 8685.
(41) Pei, Q.; Yang, Y. *J. Am. Chem. Soc.* **1996**, *118*, 7416.
(42) Liu, B.; Gaylord, B. S.; Wang, S.; Bazan, G. C. *J. Am. Chem. Soc.* **2003**, *125*, 6705.
(43) McQuade, D. T.; Pullen, A. E.; Swager, T. M. *Chem. Rev.* **2000**, *100*, 2537.
(44) Bard, A. J.; Faulkner, L. A. *Electrochemical Methods—Fundamentals and Applications*; Wiley: New York, 1984.
(45) Janietz, S.; Bradley, D.; Grell, M.; Giebeler, C.; Ibnbasekara, M.; Woo, E. P. *Appl. Phys. Lett.* **1998**, *73*, 2453.
(46) Neher, D. *Macromol. Rapid Commun.* **2001**, *22*, 1365.
(47) Jiang, X.; Liu, S.; Liu, M. S.; Herguth, P.; Jen, A.; Fong, H.; Sarikaya, M. *Adv. Funct. Mater.* **2002**, *12*, 745.
(48) Müller, D. C.; Braig, T.; Nothofer, H.; Arnoldi, M.; Gross, M.; Scherf, U.; Nuyken, O.; Meerholz, K. *Chem. Phys. Chem.* **2000**, *4*, 207.
(49) Belletete, M.; Beaupre, S.; Bouchard, J.; Blondin, P.; Leclerc, M.; Durocher, G. *J. Phys. Chem. B* **2000**, *104*, 9118.

MA050807H